Avalanche dynamics of granular materials under the slumping regime in a rotating drum as revealed by speckle visibility spectroscopy

H. Yang,[1,2] R. Li,[1] P. Kong,[3] Q. C. Sun,[4] M. J. Biggs,[2,5] and V. Zivkovic[6,*]

[1]*School of Optical-Electrical and Computer Engineering, Shanghai Key Lab of Modern Optical System, and Engineering Research Center of Optical Instrument and System, Ministry of Education, University of Shanghai for Science and Technology, Shanghai 200093, China*

[2]*School of Chemical Engineering, The University of Adelaide, SA, 5005, Australia*

[3]*Foundation department, Shanghai Medical Instrumentation College, Shanghai 200093, China*

[4]*State Key Laboratory for Hydroscience and Engineering, Tsinghua University, Beijing 100084, China*

[5]*School of Science, Loughborough University, LE11 3TU, United Kingdom*

[6]*School of Chemical Engineering and Advanced Materials, Newcastle University, NE1 7RU, United Kingdom*

(Received 9 December 2014; published 30 April 2015)

We used speckle visibility spectroscopy to measure the time-resolved dynamcis of avalanching down the inclined surface of a granular material in a half-full rotating drum operating in the slumping regime. The distribution of the avalanche period, t_d, rest time between them, t_r, and peak particle velocity fluctuation, δv_p^2, are all normally distributed. While the distributions of the two times at the top and bottom of the free surface are very similar, the particle velocity fluctuation is greater at the bottom of the free surface than at the top. The rest time is observed to be inversely related to the drum speed. Combining this with the relation of t_r and the difference of the upper and lower angle of repose for the granular material, $\Delta\theta$, we find that the latter decreases linearly with increasing rotational speed. We also observe that t_d increases in a linear fashion with the drum speed. Using the relation of t_r and the distance that particles have to move during an avalanche, we further find that a new scaling relation of the mean number of avalanches required to traverse the free surface with drum speed. We find that the slumping frequency increases with the rotating speed before becoming constant in the slumping-to-rolling transition region. Finally, we find that the average peak of the fluctuation speed of the avalanche, δv_p^2, increases linearly with the drum speed.

DOI: 10.1103/PhysRevE.91.042206 PACS number(s): 45.70.Ht, 47.57.Gc, 42.62.Fi

I. INTRODUCTION

Granular flows in rotating drums are of wide interest not only as model systems in the study of the physics of granular media, but also because of their extensive use in the chemical, minerals, pharmacutical, and food processing contexts where they are employed to effect processes as diverse as mixing and granulation. It is well known that as the drum rotational speed increases, the granular flow takes on one of a number of regimes [1], including slumping, which occurs at lower rotational speeds and is of wide relevance to industial processes as well as environmental problems such as dune migration, sediment transport, landslides, and avalanches [2,3]. In the slumping regime, the granular bed at the bottom of the tumbler rotates as a rigid body with the rotating drum wall until it reaches the upper angle of repose, θ_U, at which point the grains on the bed free surface begin to slide down the inclined surface in the form of an avalanche as illustrated in Fig. 1. The grains continue to flow down the bed-free surface until the slope of the surface drops below a lower angle of repose, θ_L. The cyclical process of elevation of the bed and slumping of the free surface layer, termed the "slump cycle," depends on the upper and lower angles of repose and their variation with the rotating speeds of the drum. While there is some appreciation of typical values of θ_U and θ_L [4,5], the small difference between them (1–3°) and the large measurement errors relative to this (0.5°) means their variation with drum rotational speed is not well understood. Image analysis has suggested that the difference between the angles, $\Delta\theta$, for dry noncohesive particles is constant or weakly variant with rotational speed [1,6,7]. Tegzes *et al.* [8], on the other hand, found that the difference in angles for a wet granular material decreased to a critical value with increasing rotational speed. Despite this experimental work, however, no mathematical model or scaling relation has been determined for the difference between the angles of repose.

A number of mathematical models for slumping of granular materials in rotating drums have been proposed over the years. They are, however, not without their problems. The models of Henein *et al.* [9] and other related models [3,10] for predicting the slumping and rolling transitions, for example, assume the grains fall from wedge OAB to OA′B′ in Fig. 1 in a single avalanche. However, this is in conflict with the work of Lim *et al.* [11], who observed via positron emission particle tracking (PEPT) that the number of steps the particles require to travel from the top to the bottom of the bed-free surface decrease to one with the increasing speed. Another similar geometrical model, termed the "wedge model" [12,13], was developed on the assumption of one avalanche for a half-full bed, but more than one avalanche otherwise as in, for example, the PEPT-based study of Lim *et al.* [11]. While another model of Ding *et al.* [14] avoids this assumption, it assumes the avalanche duration is independent of the rotational speed, which also conflicts with experimental evidence [1,3].

There are a range of experimental methods available for the study of the granular microdynamics in rotating drums, including particle image velocimetry [15], particle tracking velocimetry [16,17], PEPT [11,18], magnetic resonance imaging

*Vladimir.zivkovic@ncl.ac.uk

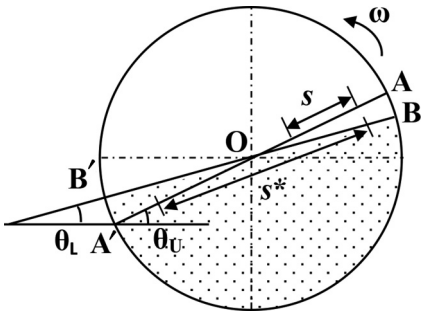

FIG. 1. Schematic of granular material in the rotating drum under the slumping regime.

[19,20], and x-ray microtomography [21]. Some of these are restricted to two components of motion (PIV and PTV) while the remainder can only resolve the granular dynamics to a fine scale with relatively poor temporal resolution or *vice versa*. In contrast, diffusing-wave spectroscopy (DWS) [22], a dynamic light-scattering (DLS) technique, is able to resolve the average of the three components of motion of grains in dense systems with spatialtemporal resolutions [23,24] that allow the probing of the microdynamics of avalanches. However, as it is based on temporal correlation functions calculated as a time average, it is not appropriate when bulk motion such as drum rotation is present. In such cases, the related method of speckle visibility spectroscopy (SVS) [25–27] can be used.

In this paper, we report the SVS-based study of the avalanching of grains in a rotating drum under the slumping regime. After introducing the SVS method and the rotating granular drum flow system to which it has been applied here, we report in detail on the comparison of the statistics of the temporal avalanches that occur at the top and bottom of the inclined free surface of the granular material. The statistics considered include the avalanche duration, rest time, frequency and peak fluctuation velocity, and the average number of avalanches a particle experiences as it transition from the top to the bottom of the inclined free surface. This data is used to assess the existing models for slumping of granular materials in rotating drums and suggest improved versions of the models.

II. EXPERIMENTAL METHOD

A. Drum system

The results reported here were obtained in a drum, Fig. 2, whose inner diameter, D, and length, L, are 142 and 200 mm, respectively. The drum, which is made of clear plexiglass to permit optical access, was half filled with granular material and placed on a pair of rollers turned by a DC motor in the range of 0.1–0.37 revolutions per minute (RPM). Two points on the free surface of the granular material were studied here: the primary point, denoted by Ⓐ in Fig. 2, was located at the top of the inclined surface, while the other point, denoted by Ⓑ, was located at the bottom of this surface. The tangential velocities for these two measurement points are between 0.52 and 1.94 mm/s for the range of angular velocities used (0.1 to 0.37 RPM). The granular material considered in the study reported here was a dry, cohesionless glass particulate material

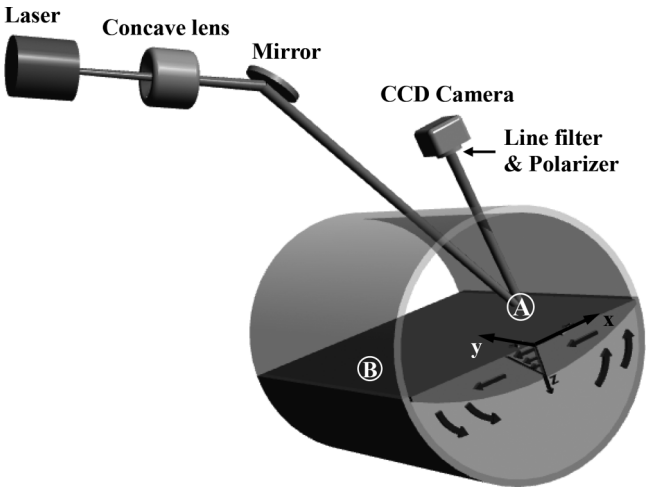

FIG. 2. Schematic of the experimental setup. The points Ⓐ ($x = 50$ mm, $y = 100$ mm) and Ⓑ ($x = -50$ mm, $y = 100$ mm) were the focus of the SVS analysis reported here.

whose size distribution spanned the 500–600 μm diameter range (Yanmoo, Guangdong, China).

B. Angle of repose measurement

The profile images of the granular materials in the drum were recorded by a CCD camera (1024 × 1024 pixels at 50 frames/s) as shown in Fig. 3. A weight was hung alongside the drum as a plumb line so as to facilitate evaluation of the angle of repose. The upper and lower angles of repose were measured directly from snapshots just before and after an avalanche, respectively. This was done by fitting a straight line to the surface of the granular bed and comparing it to the plumb line. Average angles of repose and standard deviations were derived from measurements over ten successive slumping cycles.

C. SVS details

Speckle visibility spectroscopy involves illuminating the granular material with a monochromatic laser light beam of wavelength λ, Fig. 2. The photons emerge from the granular material after diffusing within it to form a speckle pattern that is detected by a CCD camera in the far field. In the absence of any motion of the light scatters (the particles here), each

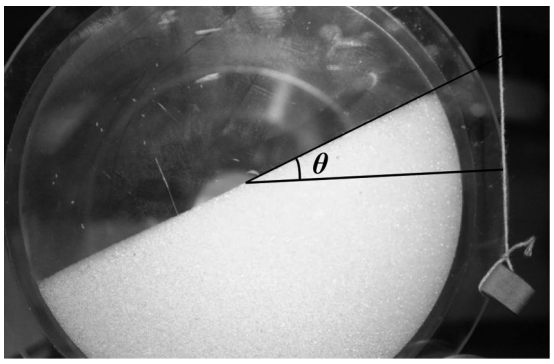

FIG. 3. Schematic of measurement of angle of repose from the profile image of grains in the drum at 0.15 RPM.

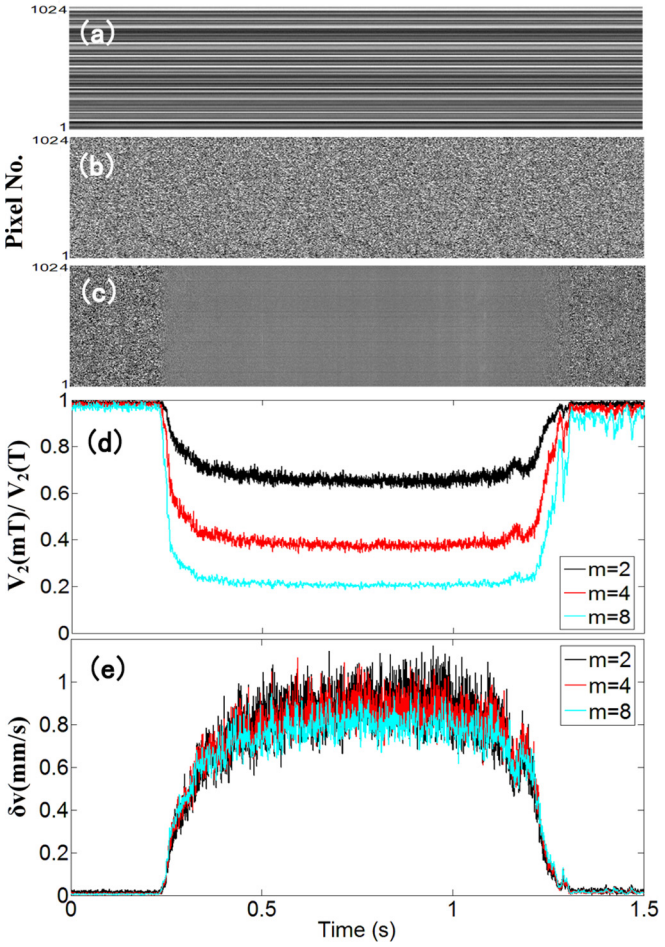

FIG. 4. (Color online) Example SVS results and analysis for glass beads in a drum: (a) intensity across the CCD pixels vs. time when the drum is stationary; (b) intensity across the CCD pixels vs. time when the drum is rotating at a speed of 0.15 RPM and no avalanche event occurs; (c) the same as (b) except an avalanche event has occurred in the period of around 0.25–1.25 s; (d) intensity variance ratio, Eq. (1), evaluated from the data in (c); and (e) root-mean-particle fluctuation velocity (δv) obtained from variance ratio.

pixel detects a constant intensity as illustrated by the example in Fig. 4(a). Motion of the scatters leads, however, to temporal fluctuations over the pixels, as illustrated by the example in Fig. 4(b). For a given exposure time, the faster the dynamics of the grains, the more the speckle image is blurred and the lower the contrast—this enables the capture of rapid changes in the granular material with time such as occurs in an avalanche as illustrated in the example of Fig. 4(c). This variation in intensity can be quantified by the variance of the intensity [25]

$$V_2(T) \propto \langle I^2 \rangle_T - \langle I \rangle^2, \tag{1}$$

where $\langle \cdots \rangle_T$ denotes the average over pixels exposed for a duration T. The proportionality constant of $V_2(T)$ is set by the laser intensity and the ratio of speckle to pixel size (i.e., it is set-up dependent). It can, however, be eliminated by considering the variance ratio $V_2(mT)/V_2(T)$, where the numerator is found from a "synthetic exposure" equal to the sum of m successive images [25]. As demonstrated in Fig. 4(d), the variance ratio equals almost one when the grains are jammed and decreases dramatically during granular collision events. For diffusely backscattered light from particles moving with random ballistic motion, whose power spectrum is Lorentzian [28,29], the theory of SVS [25] gives the variance ratio as

$$\frac{V_2(mT)}{V_2(T)} = \frac{e^{-2mx} - 1 + 2mx}{(e^{-2x} - 1 + 2x)m^2}, \tag{2}$$

where $x = (4\pi\delta v/\lambda)T$. The root mean fluctuation in the speed of the particles, $\delta v = \sqrt{\langle \delta v^2 \rangle}$, which is equal to the collision velocity and related directly to the so-called granular temperature [30], can be obtained by inverting Eq. (2), as illustrated in Fig. 4(e); note that the similarity in the speed fluctuations for different values of m indicates that the experimental method has been implemented appropriately, as the fluctuations should not depend on the exposure time [25]. The fluctuation speeds that can be detected with a particular experimental setup is dictated by the wavelength of the light used and the scan speed of the CCD camera. This makes the approach ideal for probing in detail avalanche-related phenomena in rotating tumblers.

In the SVS experimental setup used here, a laser beam of wavelength $\lambda = 532$ nm and power 300 mW was passed through a concave lens and an aperture before normally illuminating a spot of around 10 mm diameter on the inclined free surface of the granular material. A line scan CCD camera of 1024 pixels, each 14×14 μm and 8-bits deep, was placed about 350 mm away with its optical axis normal to the drum, such that the ratio of pixel to speckle size is about 0.5 [31]. A polarizer, whose direction was vertical to that of the incident laser, was used to block the poorly scattered light. A line filter was used on the CCD camera to eliminate the ambient light. The camera was operated at the expose mode of line rate of 20 KHz, giving a sample time of $T_s = 50$ μs, and an exposure time of $T = 48.5$ μs. The difference of T_s and T is resulted from the line transfer time of the camera, which is about 1.5 μs and depends on the hardware of the camera in general. The laser power was adjusted to give an average gray scale level of 50. Each measurement for a particular condition (i.e., point or drum speed) involved collecting video data for 1000 s.

D. Model for avalanching

A slumping cycle may be subdivided into two phases: (a) elevation of the bed; and (b) slumping of the free surface layer. During the first step, the rest time between two successive avalanches, t_r, equals the solid body rotation time

$$t_r = \frac{\Delta\theta\pi}{180\omega}, \tag{3}$$

where ω is the angular speed of the cylinder in $\frac{\text{rad}}{\text{s}}$.The duration of the avalanche,the second step of the cycle,can be evaluated using [9]

$$t_d = \sqrt{\frac{2s}{\text{g}(\sin\eta - \mu\cos\eta)}}, \tag{4}$$

where g is the acceleration due to gravity, η the average of the upper and lower angles of repose, $\mu = \tan\theta_L$ the friction

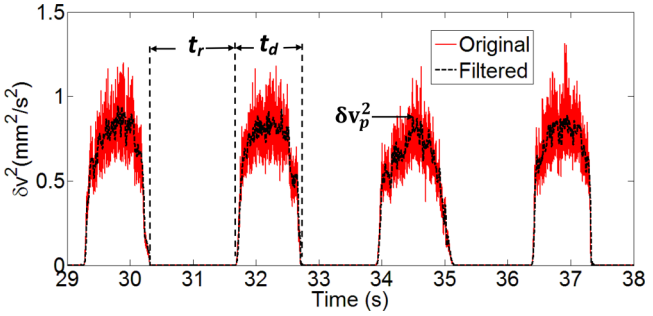

FIG. 5. (Color online) Particle fluctuation velocity, δv^2, over four slump cycles for a drum rotating at a speed of 0.15 RPM. The gray (red online) line represents the raw SVS data whilst the black dash line represents the data after being subject to a Butterworth low pass filter to reduce the noise that originates from the CCD camera.

coefficient, and s the distance that the particles travel during an avalanche as shown in Fig. 1.

III. RESULTS AND DISCUSSION

A. Avalanching statistics

Figure 5 shows the typical SVS-derived time trace of particle velocity fluctuation, δv^2, over four avalanche events at the point Ⓐ on the inclined surface of the glass particle bed at a drum at rotational speed of 0.15 RPM along with a filtered version thereof, which removes CCD camera related noise. Looking at a single avalanche event shows that the particle velocity fluctuation accelerates progressively to a maximum before similarly decelerating. The avalanche duration, t_d, rest time, t_r, and the peak of the particle velocity fluctuation, δv_p^2, can be straightforwardly measured from the filtered trace for many slumping cycles.

Figure 6 shows the comparison of the distributions of the avalanche statistics for the points Ⓐ and Ⓑ when the drum is rotating at a speed of 0.15 RPM. Figures 6(a) and 6(b) show that the rest time and avalanche duration for these two points are very similar and both normally distributed with standard deviations less than 10% of the average (see Table I). This normality combined with the relation between the rest time and difference in angles of repose in Eq. (3) indicates the latter quantity is also normally distributed. This conclusion agrees with the previous experimental study by Fischer [5]. Furthermore, using the average $t_r = 1.32$ s with the rotational speed of 0.15 RPM in Eq. (3) gives an average $\Delta\theta = 1.2^\circ \pm 0.1^\circ$, which is close to the values obtained from image analysis of our experimental setup: $\theta_L = 23.6^\circ \pm 0.5^\circ$ and $\theta_U = 24.8^\circ \pm 0.5^\circ$, leading to $\Delta\theta = 1.2 \pm 0.5^\circ$.

Using $t_d = 1.02$ s, $\theta_L = 23.6^\circ$ and $\theta_U = 24.8^\circ$ in Eq. (4) yields the average distance of particle travel during an avalanche of $s \approx 55$ mm. If particles travel in single avalanche from the top to the bottom, the mean distance particles travel directly down the inclined surface would be $s^* = 2D/3 = 95$ mm (see Fig. 1). Therefore, our result suggests that the particles experience around two avalanches on average as they travel from the top to the bottom of the drum. This is in line with the PEPT study of Lim *et al.* [11] but at odds with the single avalanche assumption in the models of Henein *et al.* [9] and others [3,10].

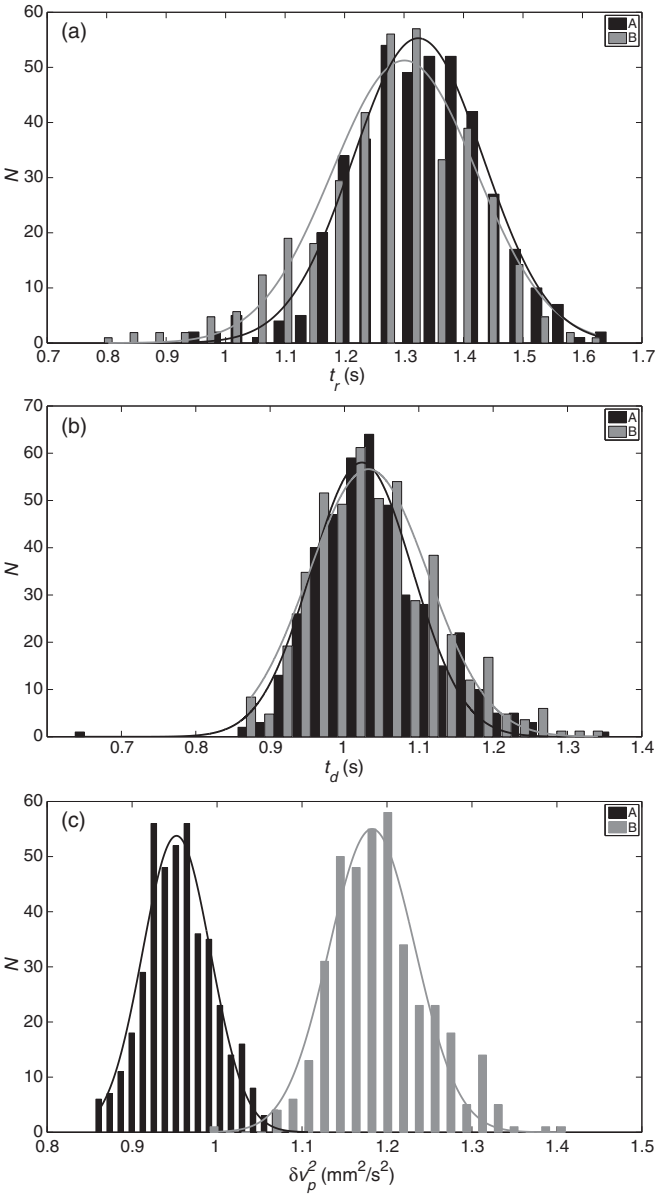

FIG. 6. The comparison of the distributions of the following obtained for points Ⓐ (black) and Ⓑ (gray) in the drum when rotating at a speed of 0.15 RPM: (a) the rest time, t_r, (b) the avalanche duration time, t_d, and (c) the peak of the particle fluctuation speed of the avalanches, δv_p^2. The data was accumulated from 424 separate avalanches events over 1000 s. The solid curves represent the best fit of a Gaussian distribution to the experimental data, with the averages and standard deviations indicated in Table I.

Figure 6(c) shows that the particle fluctuation speed of the avalanches, δv_p^2, for points Ⓐ and Ⓑ are normally distributed also, but the averages are very different. This is indicative of a much higher collision frequency for the grains at the bottom of the free surface compared to the top. It also agrees with the flow imaging analysis of granular materials in a 2D drum under the rolling regime [32,33] and discrete element modelling results [34,35].

TABLE I. The averages and standard deviations of the Gaussian distributions of the t_d, t_r, and δv_p^2.

Avalanche characteristic	Position	Average	Standard deviation
t_r	Ⓐ	1.32 s	0.11 s
	Ⓑ	1.31 s	0.12 s
t_d	Ⓐ	1.02 s	0.07 s
	Ⓑ	1.03 s	0.08 s
δv_p^2	Ⓐ	0.95 mm^2/s^2	0.04 mm^2/s^2
	Ⓑ	1.18 mm^2/s^2	0.05 mm^2/s^2

Figure 7 shows the peak of particle fluctuation velocity of the avalanche, δv_p^2, against the corresponding duration time t_d at point Ⓐ in the drum when rotating at a speed of 0.15 RPM. This indicates that these two avalanche parameters are negatively correlated: higher particle fluctuation velocity tends to lead to shorter avalanches (i.e., higher dissipation leads to faster "cooling"). This is in line with previous study of Fischer *et al.* [5], where it was observed that avalanches that start at a high angle tend to stop at a low angle in a shorter time.

Figure 8 shows the normalized power spectrum density (NPSD) of the particle fluctuating velocity, δv^2, of the granular flow and the best Gaussian fit to the peak data. It is clear that the temporal particle fluctuating velocities of the granular materials in the drum is periodic, with the first harmonic being around 0.42 Hz (equal to a period of 2.38 s), which corresponds very well with the average period of the avalanches (i.e., $t_d + t_r = 2.34$ s). This suggests that the PSD may be an easier and faster way of obtaining the avalanche period than through the analysis of the distribution of the temporal δv^2 obtained from the likes of Fig. 5.

B. Variation of avalanches statistics with drum speed

Figure 9(a) shows the comparison of the average rest times, t_r, and the average avalanche duration time, t_d, for the point Ⓐ with drum rotational speed and the related Froude number (Fr), which is defined as $\mathrm{Fr} = \omega^2 D/2g$. As can be seen from this figure, the average rest time under the slumping regime

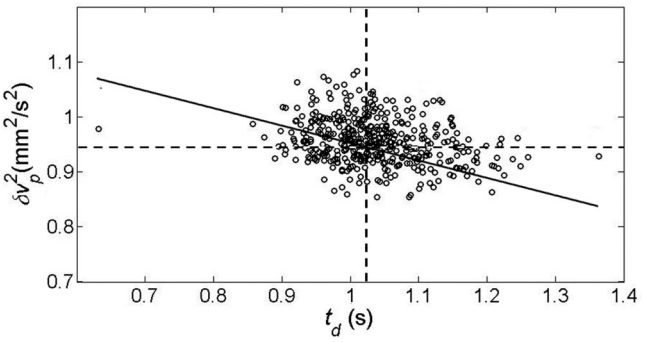

FIG. 7. The peak of the particle fluctuation velocity, δv_p^2, vs. corresponding duration time, t_d, for each of the 424 avalanches observed at point Ⓐ in the drum when rotating at a speed of 0.15 RPM (open circle) and the fit to this data (solid line). The horizontal and vertical dashed line represents the mean δv_p^2 and t_d.

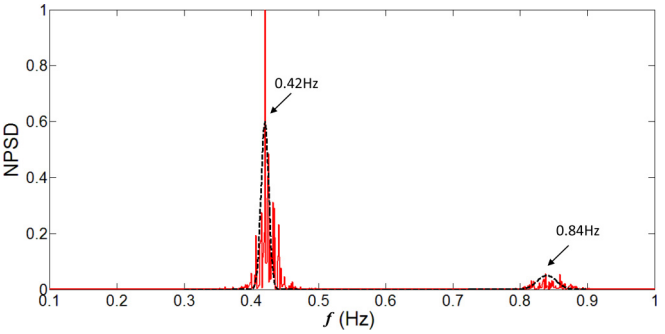

FIG. 8. (Color online) Normalized power spectrum density of the δv^2 represented by gray (red online) curve measured in 1000 s, with frequency, f, reduced from 0.1 to 1 Hz. The black dash curve represents the Gaussian fit to the peaks of the data.

decreases with increasing drum rotational speed according to (coefficient of determination, $R^2 = 0.99$)

$$t_r = 0.024/\omega - 0.23. \tag{5}$$

Using this in Eq. (3) indicates that $\Delta\theta$ is not constant but, rather, decreases linearly with rotational speed as shown in Fig. 9(b). This has an important implication for the wedge model [12,13], where this parameter is the only input (i.e., the method here can form the basis for application of this model to study influence of rotational speed on solid mixing). Figure 9(a) shows that the duration, t_d, increases linearly with the rotating speeds ($R^2 = 0.99$) as per

$$t_d = 9.36\omega + 0.87. \tag{6}$$

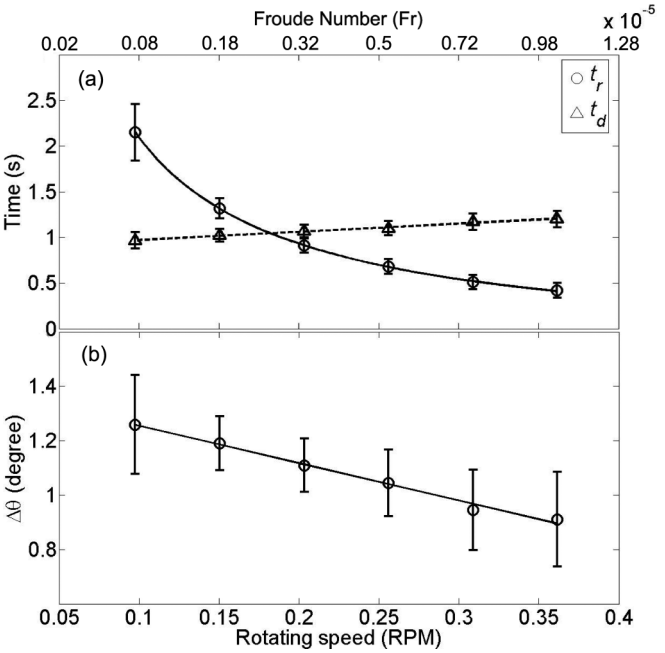

FIG. 9. (a) The comparison of the average rest time, t_r (open circles), and the average avalanche duration time, t_d (triangle), vs. drum speed and Froude number, along with the best reciprocal law to t_r (solid line), and line fit to the t_d (dash line) for point Ⓐ. (b) The variation of $\Delta\theta$ with the rotating speeds. Error bars are standard deviations of the distribution of these parameters.

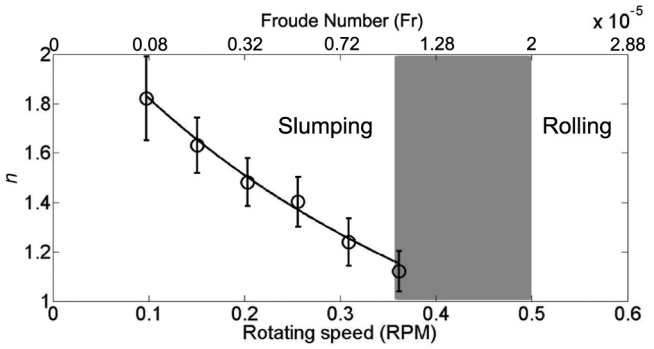

FIG. 10. The variation with drum rotational speed (in the form of Froude number) of the average number of avalanches experienced by particles as they travel from the top to the bottom of the free surface, n, (open circle) as determined from Eq. (7). Gray area represents expected transition region according to previous study of similar systems [1,3,36].

Using this with Eq. (4) gives the following expression for the number of steps the particles require to travel from the top to the bottom of the bed-free surface:

$$n = \frac{s^*}{s} = \frac{s^*}{0.5g(\sin\eta - \mu\cos\eta)(9.36\omega + 0.87)^2}. \quad (7)$$

Figure 10, which shows this function for $\eta = 24.2^\circ$ and $\mu = \tan 23.6^\circ$ [8], shows that the average number of avalanches experienced by a particle as it moves from the top to the bottom of the inclined surface in the tumbler studied here varies from around two at the lowest speed considered to nearly one at the highest speed.

Mellmann [3] argues that the slumping-to-rolling transition occurs when $t_r = t_d$, which corresponds to when the shear wedge OAB in Fig. 1 can empty itself as fast as it is filled anew. Figure 9(a) shows that this simple criterion is satisfied at about 0.18 RPM. This is, however, at odds with the visual observations here, where the slumping regime prevailed up to about 0.38 RPM, the highest rotation speed accessible with the apparatus used here. This discrepancy may have its origins in the assumption that a particle requires to undergo just one avalanche to pass from the top to the bottom of the free surface, which is at odds with our experiment as well as that of others [11].

More generally, the literature [1,3,36] suggests the slumping-to-rolling transition will occur for Froude numbers between 1×10^{-5} to 2×10^{-5}, which is shown as a gray area in Figs. 10 and 11. Interestingly, this figure indicates that the average number of avalanches experienced by particles as they travel from the top to the bottom of the bed approaches unity in this region. However, the transition from slumping-to-rolling regime is fuzzy [36], with documented temporal intermittency between discrete avalanche and continuous flow at the transition regime [37]. Further studies are planned in this region to elucidate if this parameter does indeed become unit at the start of this transition region.

Figure 11 shows the variation of the slumping frequency [1], f_{sl}, the inverse of the sum of t_r and t_d as obtained by the PSD, increases with the rotating speeds. The trend of the frequency is very similar to the measurement by Henein *et al.* [1]. Using the relationship that $f_{sl} = 1/(t_r + t_d)$, and Eqs. (5)

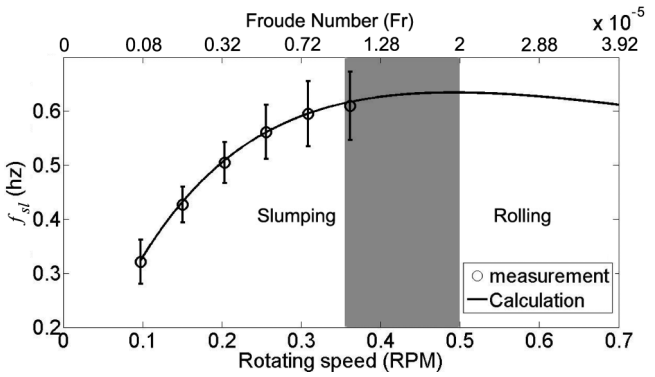

FIG. 11. The slumping frequency, f_{sl} (open circle), vs. rotating speed. The solid line represents the calculated frequency using Eq. (8) with R square of 0.99 to the measured value. Error bars are standard deviations of the slumping frequency. Gray area represents expected transition region according to previous study of similar systems [1,3,36].

and (6), we obtain the relation of f_{sl} with the rotating speed as

$$f_{sl} = \frac{1}{9.36\omega + 0.024\omega^{-1} + 0.64}, \quad (8)$$

which is represented by the solid line in Fig. 11. It is clear that the calculated variation of the slumping frequency with the rotating speeds fits our measurements very well. Extrapolating this relationship indicates that the slumping frequency should become constant in the transition region. Further studies are planned in this region to confirm this finding.

Figure 12 shows that the comparison of the averages of the peak of particle fluctuation speed of avalanche, $\langle \delta v_p^2 \rangle$, from all the avalanches over 1000 s with the rotating speeds for the point Ⓐ and Ⓑ. It is clear that both of the $\langle \delta v_p^2 \rangle$ increases linearly ($R^2 = 0.99$) with rotational speed,

$$\langle \delta v_p^2 \rangle = k\omega + c, \quad (9)$$

where $k = 3.25$ and 4.11 and $c = 8.6$ and 10.51 for points Ⓐ and Ⓑ, respectively. This shows that the instantaneous particle fluctuation speed of the granular flow during avalanche

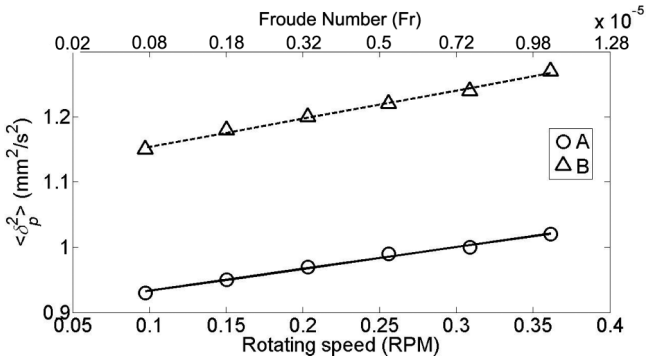

FIG. 12. Comparison of the average of the peak of particle fluctuation speed, $\langle \delta v_p^2 \rangle$, of the avalanches for the points Ⓐ (top) and Ⓑ (bottom) vs. the rotating speeds and Froude number. The solid and dash line represents the best line fitting to the data for the points Ⓐ (top) and Ⓑ (bottom), respectively.

increases linearly with the drum speeds, which is in line with our previous study [21] that the average granular temperature scales with forcing velocities in various granular systems, although these systems were time-independent, while it is time-dependent here.

IV. CONCLUSION

In this paper we used SVS to measure the time-resolved dynamics of avalanching of granular material down the surface of a granular bed in a rotating drum. These experiments lead to the following observations:

(1) The avalanche processes at the top and bottom of the free surface are periodic with a duration, t_d, and rest time, t_r, that are uniformly distributed with similar means and standard deviations. These avalanche characteristics appear to not vary with position on the inclined surface.

(2) The peak particle velocity fluctuation, δv_p^2, of the avalanches are similarly normally distributed, but the average at the bottom is substantially greater than that at the top of the free surface. This avalanche characteristic appears to vary substantially with position on the inclined surface.

(3) The rest time between avalanches, t_r, decreases with increasing rotational speed. Combining this observation with the relation of t_r suggested by the model of Henein [9] leads to observation that the difference in the upper and lower angles of repose, $\Delta\theta$, decreases linearly with increasing rotational speed.

(4) The avalanche duration, t_d, increases linearly as a function of the drum speeds. Using the Henein *et al.* [9] relation for t_r and the distance that particles move during an avalanche, a scaling relation between the mean number of avalanches required to traverse the free surface and the drum speed is isolated.

(5) The commonly used criterion for transitioning from the slumping to the rolling regime, namely when $t_r = t_d$, appears to be incorrect, probably due to incorrect assumption that a particle experiences just one avalanche as it transitions from the top to the bottom of the bed free surface in the drum.

(6) The slumping frequency increases with the rotating speed before becoming constant in the transition region between slumping and rolling flow.

(7) The averages of the peak fluctuation speed of the avalanche, δv_p^2, increases linearly with the rotational speed of the drum.

ACKNOWLEDGMENTS

This work has been supported by Innovation Program of Shanghai Municipal Education Commission (15ZZ072), the fund for young college teachers by Shanghai Municipal Education Commission (zzslg2040), Hujiang Foundation of China (C14002).

[1] H. Henein, J. P. Brimacombe, and A. P. Watkinson, Metal. Trans. B **14**, 191 (1983).
[2] G. Seiden and P. J. Thomas, Rev. Mod. Phys. **83**, 1323 (2011).
[3] J. Mellmann, Powder Technol. **118**, 251 (2001).
[4] H. M. Jaeger, C.-h. Liu, and S. R. Nagel, Phys. Rev. Lett. **62**, 40 (1989).
[5] R. Fischer, P. Gondret, B. Perrin, and M. Rabaud, Phys. Rev. E **78**, 021302 (2008).
[6] X. Y. Liu, E. Specht, and J. Mellmann, Powder Technol. **154**, 125 (2005).
[7] C. M. Dury, G. H. Ristow, J. L. Moss, and M. Nakagawa, Phys. Rev. E **57**, 4491 (1998).
[8] P. Tegzes, T. Vicsek, and P. Schiffer, Phys. Rev. Lett. **89**, 094301 (2002).
[9] H. Henein, J. K. Brimacombe, and A. P. Watkinson, Metal. Trans. B **14**, 207 (1983).
[10] X. Y. Liu, E. Specht, and J. Mellmann, Chem. Eng. Sci. **60**, 125 (2005)
[11] S. Y. Lim, J. F. Davidson, R.N. Forster, D. J. Parker, D. M. Scott, and J. P. K. Seville, Powder Technol. **138**, 25 (2003).
[12] G. Metcalfe, T. Shinbrot, J. J. McCarthy, and J. M. Ottino, Nature **374**, 39 (1995).
[13] S. E. Cisar, J. M. Ottino, and R. M. Lueptow, AIChE J. **53**, 1151 (2007)
[14] Y. L. Ding, R. Forster, J. P. K Seville, and D. J. Parker, Powder Technol. **124**, 18 (2002)
[15] S. Warr, G. T. H. Jacques, and J. M. Huntley, Powder Technol. **81**, 41 (1994).
[16] N. Jain, J. M. Ottino, and R. M. Lueptow, Phys. Fluids **14**, 572 (2002).
[17] N. A. Pohlman, J. M. Ottino, and R. M. Lueptow, Phys. Rev. E **80**, 031302 (2009).
[18] D. J. Parker, A. E. Dijkstra, T. W. Martin, and J. P. K. Seville, Chem. Eng. Sci. **52**, 2011 (1997).
[19] M. Nakagawa, S. A. Altobelli, A. Caprihan, E. Fukushima, and E. K. Jeong, Exp. Fluids **16**, 54 (1993).
[20] K. Yamane, S. A. Altobelli, T. Tanaka, and Y. Tsuji, Phys. Fluids **10**, 1419 (1998).
[21] G. T. Seidler, G. Martinez, L. H. Seeley, K. H. Kim, E. A. Behne, S. Zaranek, B. D. Chapman, S. M. Heald, and D. L. Brewe, Phys. Rev. E. **62**, 8175 (2000).
[22] D. J. Pine, D. A. Weitz, P. M. Chaikin, and E. Herbolzheimer, Phys. Rev. Lett. **60**, 1134 (1988).
[23] V. Zivkovic, M. J. Biggs, D. H. Glass, and L. Xie, Adv. Powder Technol. **20**, 227 (2009).
[24] V. Zivkovic, M. J. Biggs, and D. H. Glass, Phys. Rev. E. **83**, 031308 (2011).
[25] R. Bandyopadhyay, A. S. Gittings, S. S. Suh, P. K. Dixon, and D. J. Durian, Rev. Sci. Instr. **76**, 093110 (2005).
[26] A. R. Abate, H. Katsuragi, and D. J. Durian, Phys. Rev. E. **76**, 061301 (2007).
[27] H. Katsuragi, A. R. Abate, and D. J. Durian, Soft Matter **6**, 3023 (2010).
[28] P. A. Lemieux and D. J. Durian, J. Opt. Soc. Am. A **16**, 1651 (1999).
[29] P. A. Lemieux and D. J. Durian, Appl. Optics **40**, 3984 (2001).
[30] S. Ogawa, in *Proceedings of the US-Japan Seminar on Continuum-Mechanical and Statistical Approaches in the*

Mechanics of Granular Materials, edited by S. C. Cowin and M. Satake (Gakujutsu Bunken Fukyukai, Tokyo, 1978), pp. 208–217.

[31] S. J. Kirkpatrick, D. D. Duncan, and E. M. Wells-Gray, Opt. Lett. **33**, 2886 (2008).

[32] S. C. du Pont, R. Fischer, P. Gondret, B. Perrin, and M. Rabaud, Phys. Rev. Lett. **94**, 048003 (2005).

[33] H. T. Chou and C. F. Lee, Granular Matter **11**, 13 (2009).

[34] R. Y. Yang, R. P. Zou, and A. B. Yu, Powder Technol. **130**, 138 (2003).

[35] R. Y. Yang, A. B. Yu, L. McElroy, and J. Bao, Powder Technol. **188**, 170 (2008).

[36] S. W. Meier, R. M. Lueptow, and J. M. Ottino, Adv. Phys. **56**, 757 (2007).

[37] R. Fischer, P. Gondret, and M. Rabaud, Phys. Rev. Lett. **103**, 128002 (2009).